Journal of Integrative Neuroscience

J. Integr. Neurosci. **2026**; 25(3): 49083
https://doi.org/10.31083/JIN49083

Original Research

Distinguishing Interictal Neuromagnetic Activity in Migraine With and Without Aura: A Resting-State Magnetoencephalography Study

Di Wu[1,†], Hongxing Liu[1,†], Zhiyuan Zhou[2], Yuanwen Yu[1], Qiqi Chen[3], Xiaoshan Wang[1,*]

[1]Department of Neurology, The Affiliated Brain Hospital of Nanjing Medical University, 210029 Nanjing, Jiangsu, China
[2]Department of Neurology, Shanghai General Hospital, 200235 Shanghai, China
[3]Magnetoencephalography Center, The Affiliated Brain Hospital of Nanjing Medical University, 210029 Nanjing, Jiangsu, China
*Correspondence: lidou2005@126.com (Xiaoshan Wang)
[†]These authors contributed equally.
Academic Editor: Bettina Platt
Submitted: 14 December 2025 Revised: 22 January 2026 Accepted: 3 February 2026 Published: 24 March 2026

Abstract

Background: Migraine with aura (MwA) and migraine without aura (MwoA) are believed to have distinct pathophysiological mechanisms. However, differences in their neuromagnetic activity are currently unclear. To address this knowledge gap, this study employed magnetoencephalography (MEG) to examine alterations in magnetic source strength and functional connectivity (FC) between MwA and MwoA patients. **Methods**: Resting-state MEG data were recorded for 18 MwA and 18 MwoA patients during the interictal period and compared with 18 matched healthy controls (HCs). The spectral power and FC of the visual network were estimated using minimum norm estimation (MNE) combined with the Welch technique and corrected amplitude envelope correlation. **Results**: Spectral power analysis revealed distinct frequency-dependent alterations in MwA in the left lateral occipital cortex (LOC), bilateral lingual cortices, and right transverse temporal cortex within the theta band compared with the MwoA and HCs groups. FC analysis revealed a distinct pattern of weakened FC in MwA in the low-frequency band between the visual cortex and several key regions, including the right entorhinal cortex, right rostral anterior cingulate cortex (ACC), right superior parietal cortex (SPC), left precentral cortex, and right precuneus cortex compared with the MwoA and HCs groups. The MwoA group exhibited significantly stronger FC within the ACC-visual cortex circuit in the gamma1 band compared with the MwA and HCs groups. Several abnormal FC metrics were significantly correlated with headache attack frequency in both migraine groups. **Conclusions**: This study revealed the distinct neuromagnetic signatures of MwA and MwoA, linking specific connectivity patterns to clinical features. These findings could potentially support the development of subtype-specific, targeted neuromodulation therapies for migraine.

Keywords: migraine disorders; migraine with aura; magnetoencephalography; spectrum analysis; nerve net

1. Introduction

Migraine is a common and disabling neurological disorder that is clinically classified into two main subtypes: migraine with aura (MwA) and migraine without aura (MwoA) [1]. Aura symptoms precede headaches in up to 30% of migraine patients. Visual aura is the most common aura type and occurs in more than 90% of patients who experience aura [2]. Notably, visual aura is strongly associated with cortical spreading depression (CSD) [3]. Previous studies suggest differences between MwA and MwoA patients in terms of neuroimaging findings, neurophysiological characteristics, and treatment responses. These differences may indicate distinct pathophysiological mechanisms underlying these two migraine subtypes [4].

Previous multimodal neuroimaging and neurophysiological research has provided important evidence for distinguishing between MwA and MwoA. Structural magnetic resonance imaging (MRI) studies have identified significantly greater occipital gray matter volumes in MwA compared to MwoA [5,6]. Diffusion tensor imaging studies show that MwA is associated with stronger structural connectivity linking the left parietal and occipital lobes compared to MwoA [7], but weaker connectivity for the postcentral gyrus–insula and anterior cingulate cortex (ACC)–lateral occipital cortex (LOC) circuits [8]. Functional MRI (fMRI) studies also report differences in functional connectivity (FC) patterns between MwA and MwoA under both resting-state and task-based conditions [8]. For example, MwA patients demonstrate increased brain activation compared to MwoA patients upon visual stimulation, particularly in the visual cortex [9]. Electroencephalography (EEG) studies characterize MwA by an excess of slow and hypersynchronous alpha rhythm activity [10], heightened interictal cortical responses to sensory stimuli [11], and a more pronounced lack of habituation [12]. This evidence extends the framework of cortical hyperexcitability to implicate more widespread irregularities in neural systems governing sensory functions [13].

However, the limited temporal resolution of conventional neuroimaging techniques limits their ability to

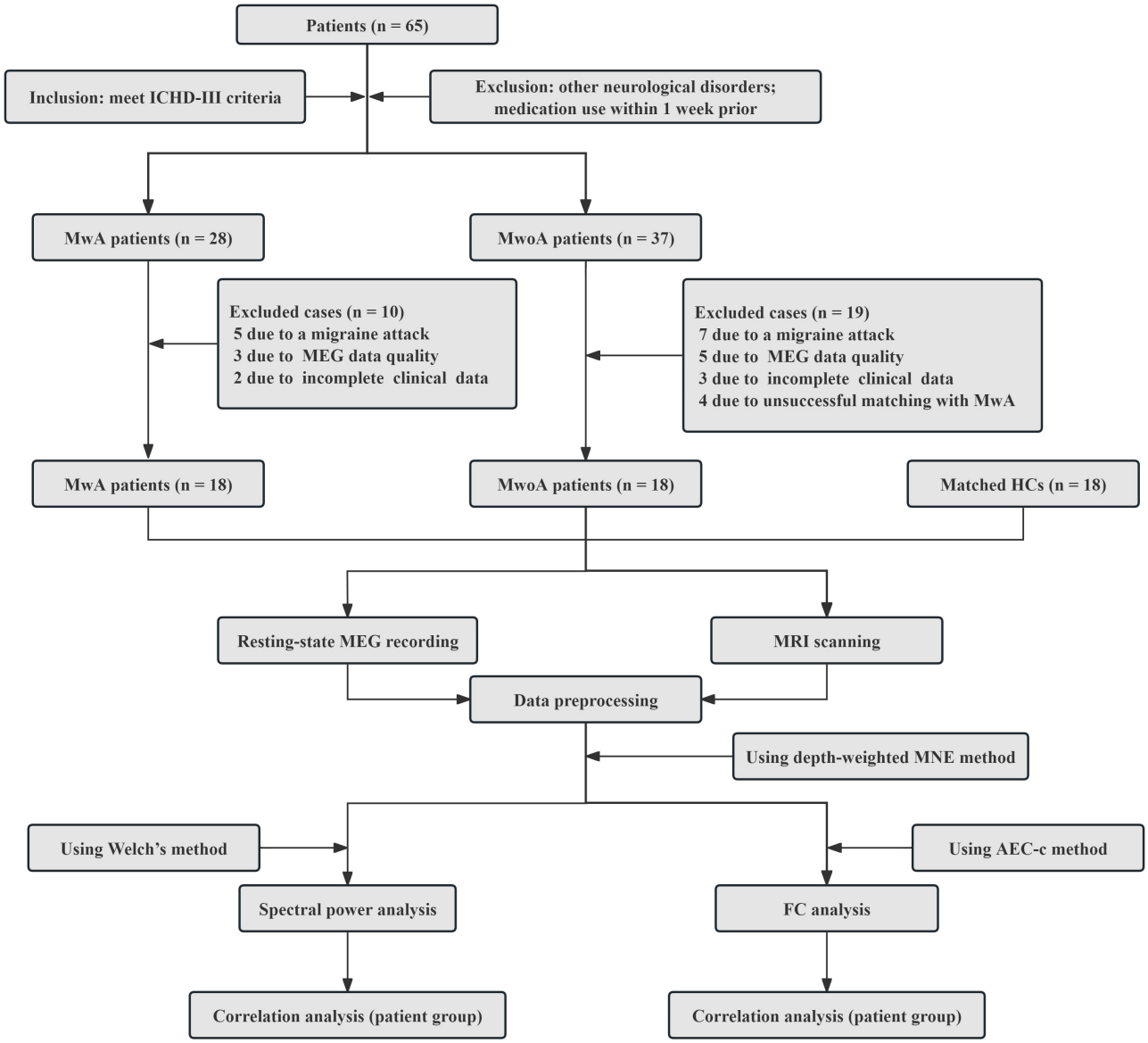

Fig. 1. Flow chart of the overall study design. ICHD-III, the International Classification of Headache Disorders, 3rd Edition; MwA, migraine with aura; MwoA, migraine without aura; MEG, magnetoencephalography; HCs, healthy controls; MRI, magnetic resonance imaging; MNE, minimum norm estimation; AEC-c, corrected amplitude envelope correlation; FC, functional connectivity.

capture transient neuroelectrophysiological activity in migraine patients. Magnetoencephalography (MEG) is an alternative approach that noninvasively records neuromagnetic activity with millisecond temporal resolution [14]. While MEG is comparable to EEG in terms of temporal resolution and spectral differentiation capability, it provides superior spatial resolution for localizing the origins of underlying neural sources, thus offering a unique approach for investigating the electrophysiological mechanisms of migraine [15]. Previous MEG studies of resting-state oscillatory power and FC in migraine patients have reported: (1) increased oscillatory power in the gamma band, with concentrations over frontal and temporal regions; (2) enhanced FC in the delta and theta bands, primarily localized to frontal and occipital areas; (3) reduced connectivity in the beta band, predominantly within regions of the pain-processing network; and (4) aberrant modulation of spontaneous resting-state activity within temporo-parieto-occipital regions [14]. However, most previous MEG studies have examined aberrant neuromagnetic activities in migraine patients compared to healthy controls (HCs), without systematic analysis of potential differences between MwA and MwoA subgroups. Whether abnormalities in neuromagnetic activity revealed by MEG can distinguish between MwA and MwoA—and whether these could serve as diagnostic biomarkers or tools for treatment evaluation—thus warrants further research.

To address this research gap, the present study utilized MEG to investigate alterations in spectral power and FC across low to high frequency bands during the resting

state in MwA patients, MwoA patients, and HCs. First, we compared resting-state spectral power changes among these three groups at the spectral power level. We then examined connectivity aberrations at the FC level between visual-related cortical areas and the whole-brain cortex across different frequency ranges in these three groups. Finally, we assessed whether spectral power and FC abnormalities observed in migraine patients correlate with clinical characteristics.

2. Materials and Methods

2.1 Study Design

This study was approved by the Medical Ethics Committee of Nanjing Brain Hospital, and all participants provided written informed consent. We recruited patients with episodic migraine from the Department of Neurology at Nanjing Brain Hospital, affiliated with Nanjing Medical University. All patients were pre-screened by neurologists specializing in headache disorders. To enhance phenotypic homogeneity, we specifically recruited patients with MwA who experienced exclusively visual aura. Initially, 28 MwA and 37 MwoA patients were recruited to account for potential exclusions due to migraine attacks or suboptimal MEG data quality. Given the challenges of recruiting well-phenotyped MwA patients, each eligible MwA patient was matched with one MwoA patient and one HC for age and sex. This matching procedure yielded a final cohort of 18 participants per group (n = 54 in total). Based on previous studies of migraine subpopulations [16] and MEG techniques [17], a sample size of 16 to 24 is sufficient for preliminary investigations of between-group differences in MEG parameters. The overall study design is presented in Fig. 1.

2.2 Participants

The inclusion criteria for patients with episodic migraine with visual aura and without aura were according to the International Classification of Headache Disorders, 3rd Edition (ICHD-III) [1]. Migraine patients were excluded if they had other neurological diseases or used prescription medications within 1 week preceding the study. HCs were recruited and matched with migraine patients in terms of age and sex. To be eligible, HCs could not have any personal history of neurologic disorders or first-degree relatives with migraine. For all participants, exclusion criteria were: (1) presence of metallic/electronic implants that may produce magnetic interference; (2) significant anxiety or poor communication that could impede the MEG session; (3) inability to remain still during data acquisition; (4) current pregnancy; or (5) claustrophobia that could prevent the requisite MRI scan. Migraine patients were scanned during the interictal period; they reported being free from headache for at least 72 h prior to MEG recording and remained so for at least 24 h afterward. Clinical characteristics of migraine patients were recorded using a structured questionnaire prior to MEG acquisition. The collected data included descriptions of aura symptoms, detailed headache characteristics, and medication usage.

2.3 MEG Recording

MEG recordings were conducted in a magnetically-shielded room at the MEG Center of Nanjing Brain Hospital using a whole-head CTF 275-channel MEG system (VSM MedTech Systems, Inc., Coquitlam, BC, Canada). Prior to data acquisition, all participants were instructed to remove any personal metallic objects to prevent interference with magnetic signals. Head position relative to the MEG sensors was monitored using three electromagnetic coils affixed to the nasion and bilateral preauricular points. These coils were activated at distinct frequencies to continuously track head movements during the recording session. MEG data were acquired in two consecutive 120 s runs at a sampling rate of 6000 Hz. Participants maintained a relaxed, supine posture during the scan with their arms at their sides. MEG data were acquired with third-order synthetic gradient noise cancellation applied to minimize environmental interference. Head position was monitored at the start and end of each recording. Data sets from sessions with head displacement $>$5 mm were excluded from analysis and an additional recording was obtained.

2.4 MRI Scanning

Structural MRI data were acquired using a 1.5 T Signa scanner (GE Healthcare, Milwaukee, WI, USA). To ensure accurate MEG-MRI co-registration, three fiducial markers were placed at anatomical locations corresponding to the positions of the electromagnetic coils used during MEG recordings. All anatomical landmarks digitized in the MEG coordinate system were subsequently identified in MRIs to establish spatial correspondence between the two neuroimaging modalities.

2.5 Data Preprocessing

All MEG analyses were performed using the publicly available, open-source Brainstorm toolkit (version 9.11.0.1769968; University of Southern California, Los Angeles, CA, USA) [18]. The following procedures were applied to remove extracranial and environmental artifacts from the MEG recordings: First, all datasets were visually inspected and segments contaminated by significant head movement or transient noise interference were excluded. Second, power line interference was removed by applying a notch filter at 50 Hz and its harmonics. Third, a 3 min empty-room recording was obtained prior to data acquisition to capture background sensor and environmental noise; this recording was used to compute the noise covariance matrix for subsequent source analysis. Finally, principal components corresponding to artifact sensor topographies were manually identified and removed via orthogonal projection [19]. For source localization, T1-weighted im-

ages were processed using FreeSurfer (version 7.1.1; Massachusetts General Hospital, Boston, MA, USA) to automatically reconstruct cortical surface models. This approach provided the precise gray/white matter boundaries required for source analysis. MEG data were analyzed in the following frequency bands: delta (2–4 Hz), theta (5–7 Hz), alpha (8–12 Hz), beta (15–29 Hz), gamma1 (30–59 Hz), and gamma2 (60–90 Hz).

Following preprocessing, quantitative quality control (QC) metrics were assessed for all included participants/retained recordings. These metrics included: (1) head displacement per participant, (2) number of artifact-contaminated data segments rejected per participant, and (3) number of artifact components removed per participant. These QC metrics were subsequently compared between the MwA, MwoA, and HC groups to confirm the absence of systematic QC differences.

2.6 Spectral Power Analysis

Cortical activation was estimated from MEG data using depth-weighted minimum norm estimation (MNE), a method with demonstrated robustness in electrophysiological source imaging [20,21]. The forward solution was computed using the overlapping sphere method with each cortical location modeled as an equivalent current dipole. The source space comprised approximately 15,000 vertices distributed across the cortical surface. The inverse operator for estimating cortical current sources from sensor-level data was constructed with the following specifications: Source orientations were constrained to be normal to the cortical surface. Depth weighting was applied to mitigate the inherent bias toward superficial sources. A regularization value ($\lambda^2 = 0.33$) was then employed to enhance numerical stability, suppress noise sensitivity, and promote spatial smoothness of the reconstructed activity. This regularization parameter balances the relative contribution of the signal and noise models, defined as the inverse of the signal-to-noise ratio (SNR). In line with the default setting in the Brainstorm toolbox and the original MNE implementation, we used an SNR value of 3 [22]. The entire cortical surface was then parcellated into 68 distinct regions of interest (ROIs) using the Desikan-Killiany atlas [23], which defines 34 ROIs per cerebral hemisphere, for the subsequent calculation of spectral power. The oscillatory power for each ROI was estimated at the source level by first computing the relative current power across all its vertices. The power spectral density (PSD) was then derived using Welch's method with 5 s Hanning windows and 50% overlap [18,24]. To facilitate cross-regional and cross-participant comparisons, the PSD in each frequency band was normalized relative to the total power across all analyzed bands as follows: Relative $PSD(f) = PSD(f)/\sum_i[\text{Total } PSD(f_i)]$, where f_i denotes a given frequency band. The numerator of this formula corresponds to the raw PSD value of that band, while the denominator represents the sum of raw PSD values across all frequency bands. This procedure yields relative PSD values bounded between 0 and 1, reflecting the proportional contribution of each frequency band to the total power. This normalization approach controls for individual differences in overall power, thereby enhancing comparisons of spectral profiles across participants and regions [24].

2.7 FC Analysis

Four bilateral visual cortical regions from the Desikan-Killiany atlas were selected for FC analysis, namely the bilateral cuneus, LOC, lingual cortex (LC) and pericalcarine cortex, resulting in a total of eight ROIs. FC between visual ROIs and all 68 brain regions was assessed using the corrected amplitude envelope correlation (AEC-c) method, which quantifies oscillatory coupling based on amplitude co-fluctuations. This method was selected due to its established test-retest reliability and robustness for characterizing FC networks [25]. To mitigate spurious connectivity arising from volume conduction and field spread, signal pairs were orthogonally aligned following an established method prior to envelope computation [26]. The amplitude envelope was derived as the absolute value of the analytic signal obtained via the Hilbert transform, reflecting amplitude fluctuations over time [27]. Specifically, the cortical source time series for each frequency band was band-pass filtered and its amplitude envelope was extracted. The amplitude envelope derived from the Hilbert transform was segmented into n non-overlapping windows of equal duration. Subsequently, the mean envelope value was computed for each window. FC between ROIs was quantified using AEC-c, which was calculated as the Pearson correlation coefficient between the averaged envelope time series from two ROIs. Higher AEC-c values indicate stronger temporal synchronization of amplitude fluctuations between regions, reflecting stronger oscillatory coupling [28,29]. Finally, AEC-c values were computed for all participants and ROI pairs, resulting in an 8×68 group-level connectivity matrix representing FC between the 8 visual seed ROIs and all 68 brain regions.

2.8 Statistical Analysis

Statistical analyses were performed using SPSS (version 27.0; IBM, Inc., Armonk, NY, USA). Normality of data distribution was assessed using the Kolmogorov–Smirnov test. Demographic variables (age, sex) and key clinical characteristics (migraine duration, migraine frequency and pain severity) were compared between the included and excluded cohorts using appropriate statistical tests (Fisher's exact test, *t*-test, or Mann-Whitney U test). As the spectral power and FC data were not normally distributed, non-parametric tests were employed. Group differences in spectral power across frequency bands and in AEC-c values (reflecting FC strength between ROI pairs) among the three groups were examined using the Kruskal–Wallis test. The Mann–Whitney U test was employed for

Table 1. Demographic and clinical characteristics of included participants.

Parameters	MwA	MwoA	HC
Gender (female/male)	9/9	12/6	11/7
Age (years) (mean ± SD)	30.67 ± 8.47	31.39 ± 7.72	30.22 ± 8.00
Handedness (left/right)	0/18	0/18	1/17
Duration of migraine history (mean ± SD)	11.81 ± 8.75	12.33 ± 8.15	/
Headache attacks per month (median and interquartile range)	3.0 (1.4, 10.0)	2.0 (1.0, 14.0)	/
Durations of migraine attacks (hours)	21.31 ± 20.81	22.72 ± 20.12	/
Headache location (unilateral/bilateral)	10/8	11/7	/
Severity of headache (VAS scale)	5.81 ± 1.04	6.47 ± 1.46	/
Associated symptoms during attack (number of participants)			
Photophobia	10	12	/
Phonophobia	10	12	/
Nausea/Vomiting	15	14	/
Prophylactic treatment in last 3 months (yes/no)	0/18	0/18	/

Abbreviations: SD, standard deviation; VAS, visual analog scale.

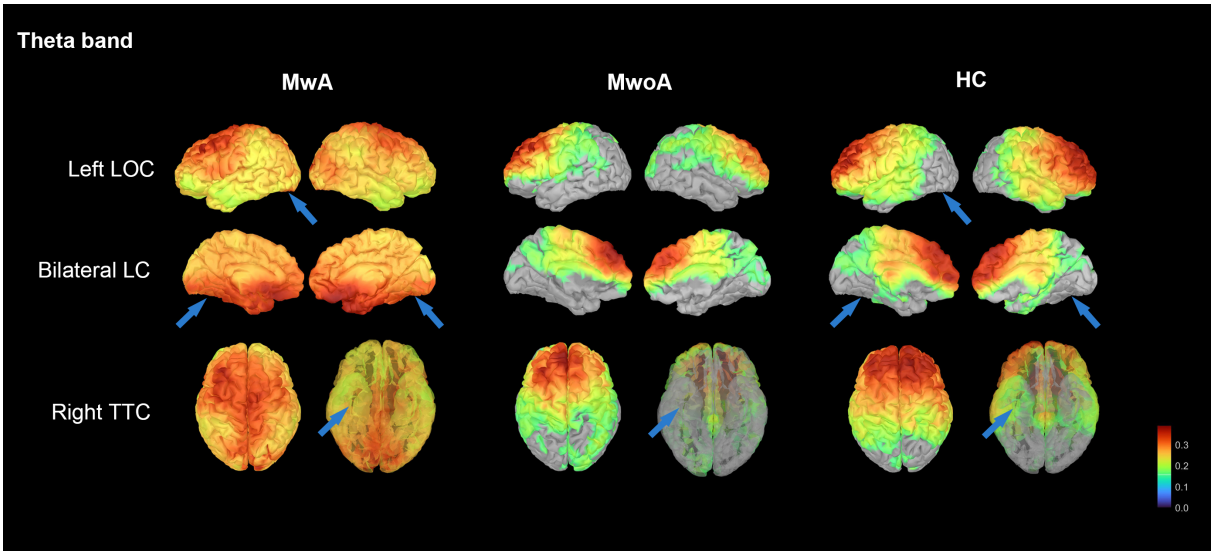

Fig. 2. Distribution of cortical activation among the MwA, MwoA, and HC groups. Spectral power distributions across the brain are shown from six distinct anatomic viewpoints (color scale: red = high power, blue = low power). Statistically significant group differences are indicated by blue arrows. A perspective view is used to visualize the deep region of the right transverse temporal cortex. LOC, lateral occipital cortex; LC, lingual cortex; TTC, transverse temporal cortex.

post-hoc pairwise comparisons. To examine potential associations, Spearman's correlation analysis was conducted between key clinical features (migraine duration, migraine frequency and pain severity) and abnormal MEG measures (spectral power and FC). A sensitivity analysis will be conducted to assess the potential adverse effects of outliers. Some of the subjects who experienced headache attacks on 14 days each month were excluded from the secondary analysis to verify the robustness of the main correlation. A two-tailed p-value < 0.05 was used as the threshold for statistical significance. For comparisons among the three groups, the significance threshold was adjusted to 0.0167 (0.05/3) using Bonferroni correction.

3. Results

3.1 Clinical Characteristics

A total of 83 participants were recruited for this study, including 28 patients with MwA, 37 patients with MwoA, and 18 HCs. Of the initial sample of 65 episodic migraine patients, several were excluded for the following reasons: 12 patients (5 MwA, 7 MwoA) reported a migraine attack within 24 h after the MEG recording; 8 patients (3 MwA, 5 MwoA) were excluded due to suboptimal MEG data quality; 5 patients (2 MwA, 3 MwoA) were excluded due to incomplete clinical assessment data for the correlation analysis; and 4 MwoA patients could not be matched to MwA patients in terms of age (±2 years) and sex. As a result, the final analysis included 54 participants that were divided

into three age- and gender-matched groups: 18 with MwA, 18 with MwoA, and 18 HCs. Detailed clinical data for the migraine groups are shown in Table 1. The migraine subgroups did not differ significantly in terms of gender distribution, age, headache history, attack frequency, and pain intensity. Comparisons between included and excluded patients within each subgroup (MwA and MwoA) revealed no significant differences (all $p > 0.05$) in demographics (age, sex) or key clinical characteristics (disease duration, attack frequency, pain intensity). Full results are presented in **Supplementary Table 1**.

3.2 Data QC Metrics

To address potential confounding due to data quality, we compared key QC metrics across groups. The median head displacement was 1.0 mm (IQR: 0.0–2.0) in the MwA group, 1.0 mm (0.0–2.0) in the MwoA group, and 1.0 mm (0.8–2.0) in the HC group, with no significant group differences ($p = 0.593$). The median percentage of rejected data segments was 15.0% (IQR: 11.5–20.0%) in the MwA group, 15.5% (12.0–18.5%) in the MwoA group, and 16.5% (12.0–20.0%) in the HC group ($p = 0.839$). The median number of artifact components removed was 2.0 (IQR: 1.0–4.0) for the MwA group, 2.0 (1.0–3.3) for the MwoA group, and 2.0 (1.0–3.3) for the HC group ($p = 0.888$). All p-values were derived from Kruskal-Wallis tests, which confirmed the absence of significant differences in data quality among the three groups.

3.3 Spectral Power

Compared to HCs and the MwoA group, the MwA group exhibited distinct frequency-dependent alterations in visual and auditory-related brain regions (Fig. 2). Group differences in spectral power were primarily concentrated in the theta frequency band. No statistically significant group differences were observed in the spectral power of the delta, beta, alpha, or gamma frequency bands.

Theta Band (5–7 Hz)

Significant group differences were observed for the spectral power of the left LOC ($p = 0.008$), left LC ($p = 0.015$), right LC ($p = 0.009$), and right transverse temporal cortex (TTC) ($p = 0.006$) (Fig. 3).

Further comparisons revealed significantly higher spectral power in the left LOC ($p = 0.001$), left LC ($p = 0.004$), and right LC ($p = 0.002$) in the MwA group compared to HCs. The MwA group also showed significantly higher spectral power in the right TTC compared to the MwoA ($p = 0.014$) and HC groups ($p = 0.003$). There were no significant differences between the MwoA and HC groups.

3.4 Functional Connectivity (FC)

FC of the visual network in the MwA and MwoA groups demonstrated distinct frequency-dependent changes compared to HCs (Fig. 4). Visual network alterations in the two migraine groups were mainly concentrated within the delta, theta, and gamma1 frequency bands. There were no statistically significant group differences in the alpha, beta, or gamma2 frequency bands.

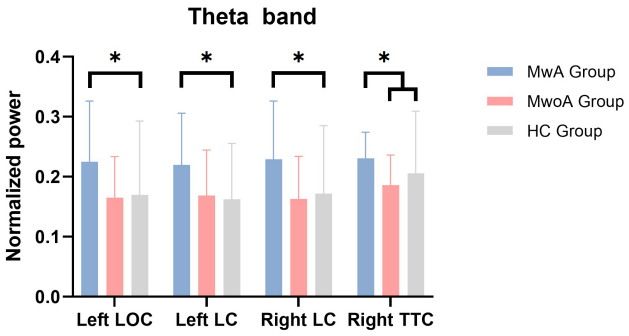

Fig. 3. Bar graph of differences in the spectral power between the MwA, MwoA, and HC groups. Statistically significant inter-group differences are indicated by asterisks (*, $p < 0.016$). Error bars show the standard error.

3.4.1 FC Alterations Specific to MwA

FC differences specific to the MwA group were primarily concentrated in the delta and theta bands. There were no significant differences between the MwA group and MwoA or HC groups in the alpha, beta, or gamma bands.

3.4.1.1 Delta Band (2–4 Hz). Significant group differences were observed for the AEC-c value of the left LOC with the right entorhinal cortex ($p = 0.007$) and right rostral ACC (rACC) ($p = 0.009$) (Fig. 5). Further comparisons showed that the MwA group had a significantly lower AEC-c value between the left LOC and right entorhinal cortex compared to the MwoA ($p = 0.010$) and HC groups ($p = 0.004$), as well as a significantly lower AEC-c value between the left LOC and right rACC compared to the MwoA ($p = 0.005$) and HC groups ($p = 0.014$). There were no significant differences between the MwoA and HC groups. There were also significant group differences in the AEC-c value between the right LC and right superior parietal cortex (SPC) ($p = 0.010$) (Fig. 5). Specifically, the MwA group had a significantly lower AEC-c value between the right LC and right SPC compared to the MwoA ($p = 0.010$) and HC groups ($p = 0.008$), whereas the MwoA and HC groups showed no significant differences.

3.4.1.2 Theta Band (5–7 Hz). Significant group differences were observed for the AEC-c value of the right LC with the left precentral cortex ($p = 0.008$) and right precuneus cortex ($p = 0.005$; Fig. 5). The MwA group showed a significantly lower AEC-c value between the right LC and left precentral cortex compared to the MwoA ($p = 0.006$) and HC groups ($p = 0.008$), as well as a significantly lower

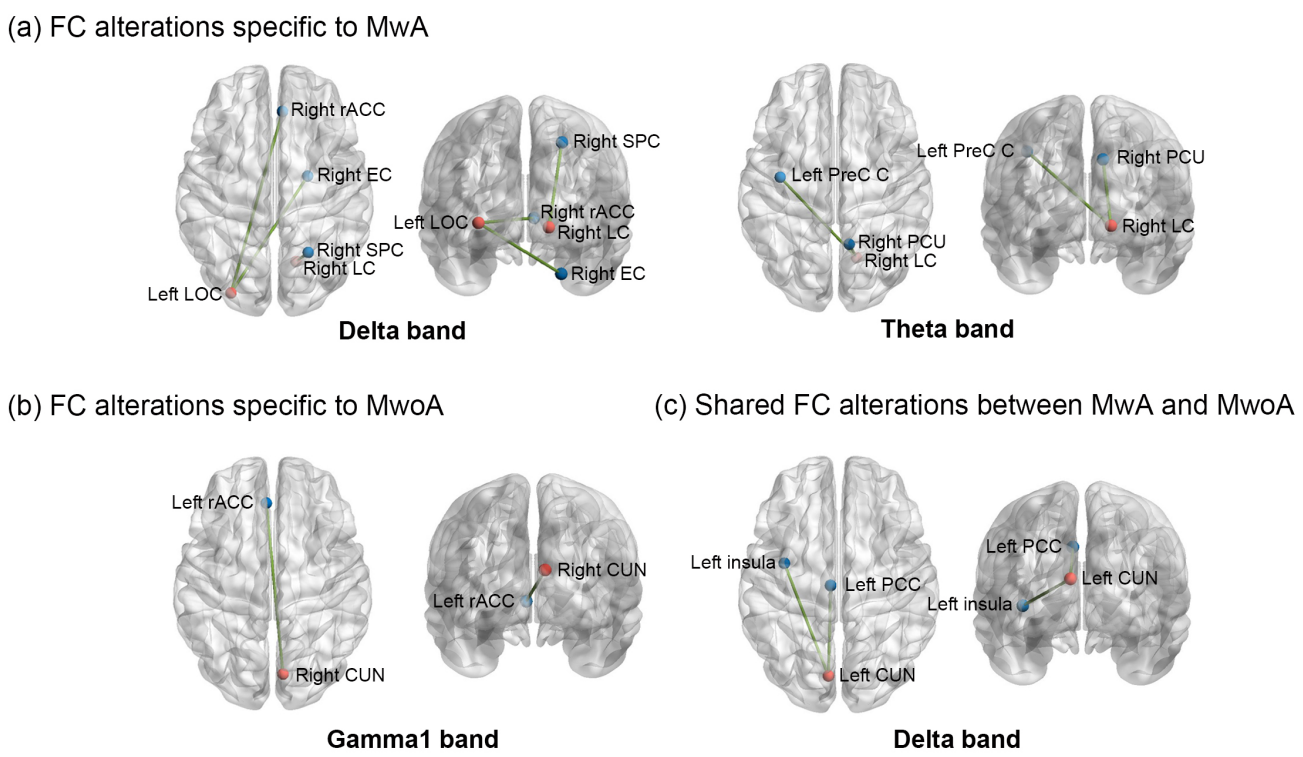

Fig. 4. Differences in FC maps between the MwA, MwoA, and HC groups. Visual cortices are represented by red spheres, while other cortical areas are denoted by blue spheres. (a) FC alterations specific to the MwA group in the delta and theta bands. (b) FC alterations specific to the MwoA group in the gamma1 band. (c) Shared FC alterations between the MwA and MwoA groups in the delta band. EC, entorhinal cortex; rACC, rostral anterior cingulate cortex; SPC, superior parietal cortex; PreC C, precentral cortex; PCU, precuneus; CUN, cuneus; PCC, posterior cingulate cortex.

AEC-c value between the right LC and right precuneus cortex compared to the MwoA ($p = 0.006$) and HC groups ($p = 0.004$). The comparison between the MwoA and HC groups revealed no significant differences.

3.4.2 FC Alterations Specific to MwoA

Differences in FC specific to MwoA were primarily concentrated in the gamma1 band. This group showed no significant differences in the delta, theta, alpha, beta, or gamma2 bands compared to the MwA and HC groups.

Gamma1 Band (30–59 Hz). Significant group differences were observed in the AEC-c value between the right cuneus and left rACC ($p = 0.010$) (Fig. 5). Further comparisons revealed a significantly higher AEC-c value between the right cuneus and left rACC in the MwoA group compared to the MwA ($p = 0.010$) and HC groups ($p = 0.007$), but no significant differences between the MwA and HC groups.

3.4.3 Shared FC Alterations Between MwA and MwoA

Differences in FC shared between the MwA and MwoA groups were primarily concentrated in the delta band. No significant differences were observed in the theta, alpha, beta, or gamma bands compared to HCs.

Delta Band (2–4 Hz). The AEC-c value of the left cuneus with the left insula cortex ($p = 0.003$) and left posterior cingulate cortex (PCC) ($p = 0.010$) showed significant group differences (Fig. 5). Specifically, the AEC-c value between the left cuneus and left insula cortex was significantly higher in the MwA ($p < 0.001$) and MwoA ($p = 0.009$) groups compared to HCs. Additionally, the AEC-c value between the left cuneus and left PCC was significantly higher in the MwA ($p = 0.011$) and MwoA ($p = 0.011$) groups compared to HCs group. There were no significant differences between the MwA and MwoA groups.

3.5 Clinical Associations

To explore clinical relevance, we examined correlations between abnormal MEG findings (spectral power and FC) and clinical migraine characteristics (migraine duration, migraine frequency and pain severity). Specific abnormal FC metrics were significantly correlated with headache attack frequency in both migraine groups (Fig. 6).

In the MwA group, the AEC-c value between the right LC and right precuneus of the theta band was negatively correlated with the frequency of headache attacks per month ($r = –0.686$, $p = 0.002$). In the MwoA group, the AEC-c value between the right cuneus and left rACC of the gamma1 band was positively correlated with the frequency

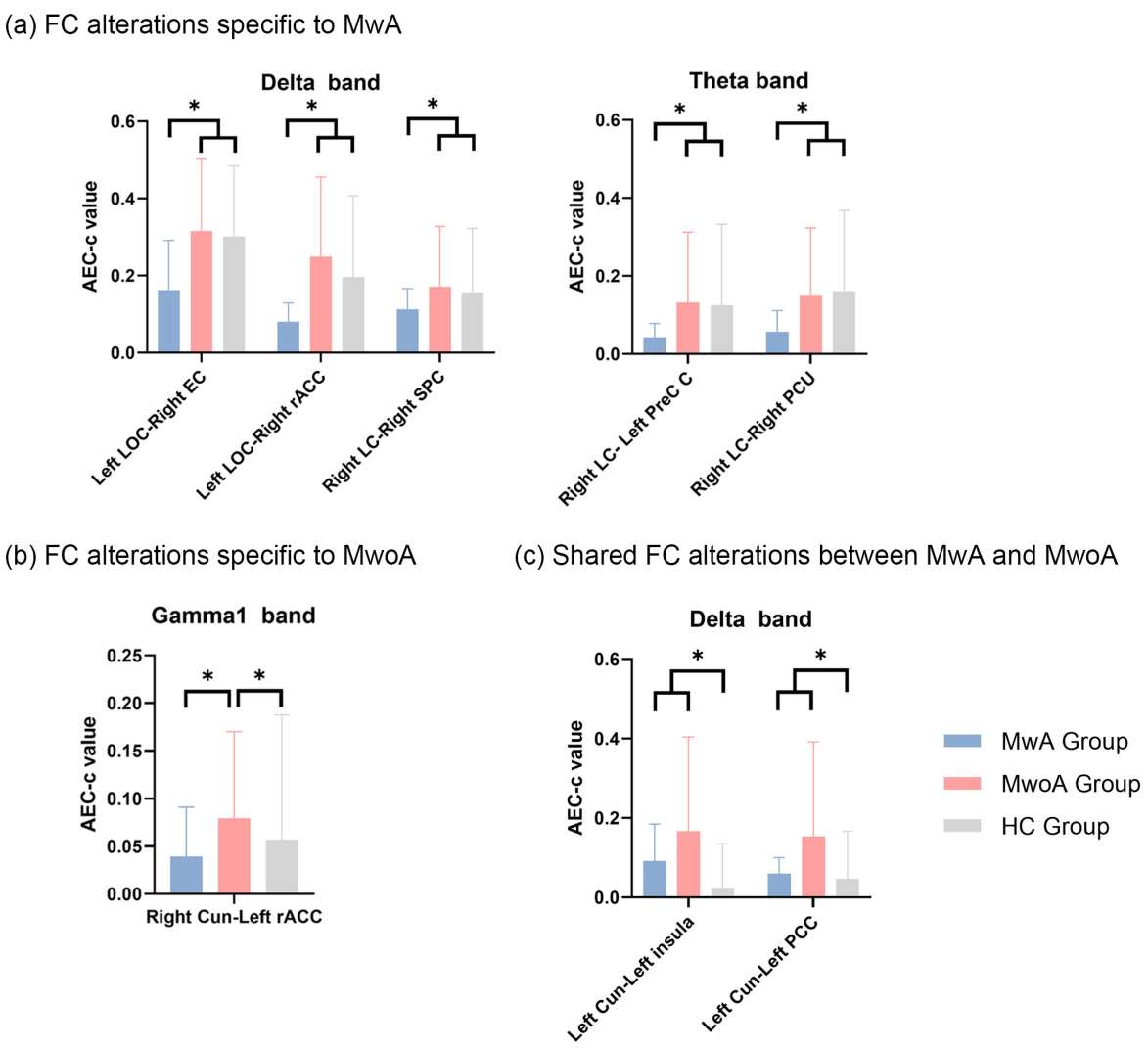

Fig. 5. Bar graph of FC differences between the MwA, MwoA, and HC groups. Statistically significant intergroup differences are indicated by asterisks (*, $p < 0.016$). Error bars show the standard error. (a) FC alterations specific to the MwA group in the delta and theta bands. (b) FC alterations specific to the MwoA group in the gamma1 band. (c) Shared FC alterations between the MwA and MwoA groups in the delta band.

of headache attack per month ($r = 0.751, p < 0.001$). In both migraine groups (MwA and MwoA), the AEC-c value between the left cuneus and left insula cortex of the delta band was positively correlated with the frequency of headache attacks per month ($r = 0.534, p < 0.001$). Abnormal spectral power demonstrated no significant correlation with any of the other key clinical migraine metrics (migraine duration, migraine frequency and pain severity).

To ensure that the main findings were not driven by participants with exceptionally high headache frequency, a sensitivity analysis was performed. We excluded a subset of participants (n = 6) who reported having headache symptoms on 14 days per month (2 from the MwA group and 4 from the MwoA group) and re-analyzed the correlation between the aberrant FC metrics and headache attack frequency. After excluding these individuals, the correlations remained statistically significant.

4. Discussion

This study utilized MEG to investigate alterations in resting-state neuromagnetic activity across high- and low-frequency bands in MwA and MwoA migraine patients, with the aim of identifying biomarkers that could distinguish these two subtypes and provide insights into their distinct pathophysiological mechanisms. Our findings revealed that MwA is characterized by unique abnormalities in both neuromagnetic source strength within the visual and auditory cortices and FC within the visual network, whereas MwoA is characterized by abnormal FC within the anterior cingulate cortex-visual cortex circuit. These differences effectively distinguish MwA from both MwoA patients and HCs and suggest a subtype-specific neurophysiological mechanism.

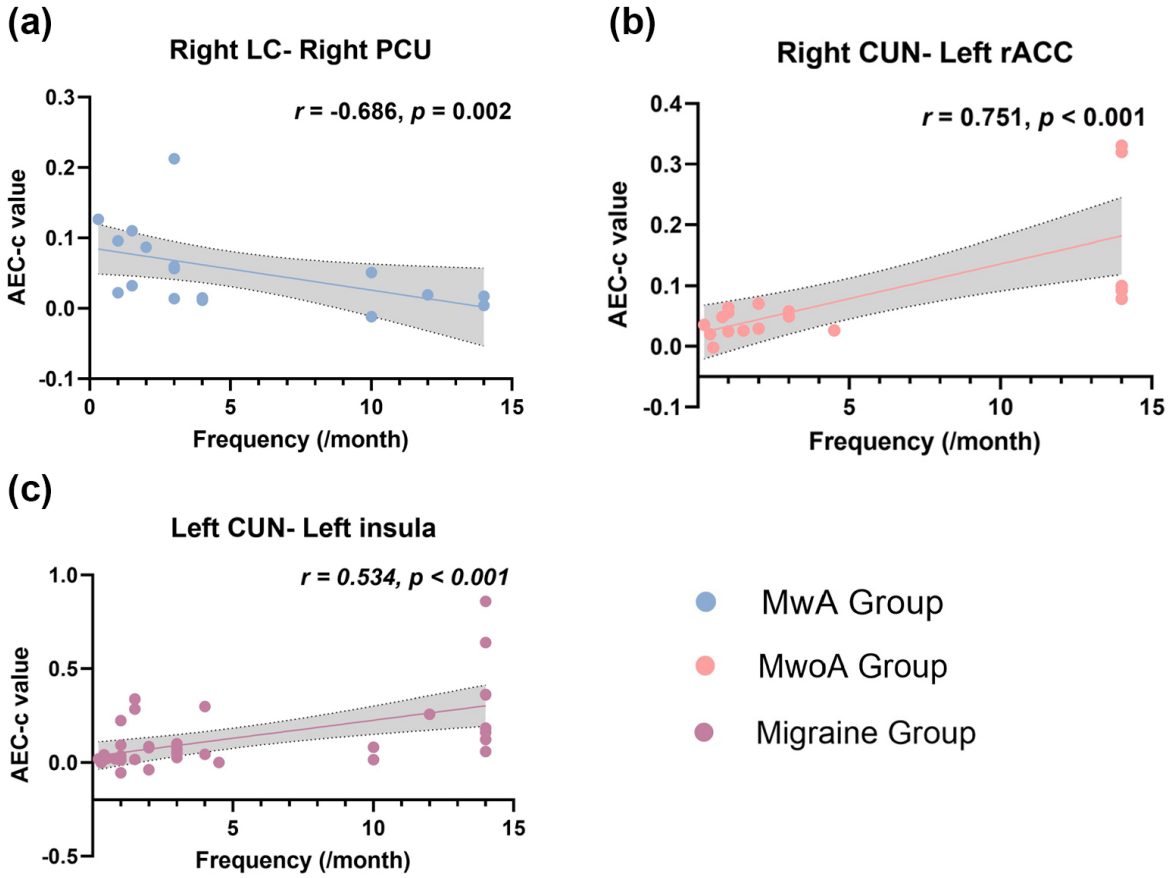

Fig. 6. Correlation between FC and headache attack frequency. (a) The AEC-c value in the MwA group between the right lingual cortex and right precuneus of the theta band was negatively correlated with the frequency of headache attack per month. (b) The AEC-c value in the MwoA group between the right cuneus and left rostral anterior cingulate cortex of the gamma1 band was positively correlated with the frequency of headache attacks per month. (c) The AEC-c value in the migraine group (MwA and MwoA group) between the left cuneus and left insula cortex of the delta band was positively correlated with the frequency of headache attacks per month.

4.1 Alterations in Neuromagnetic Activity Specific to MwA

Our findings regarding magnetic source strength indicate increased spectral power in the left LOC and bilateral LCs in the MwA group, which may reflect trait-level visual cortex hyperexcitability that could predispose individuals to aura. The LOC is crucial for visual integration and object recognition [30,31], and the LC is involved in higher-order functions like visual memory and spatial attention [32]. The occipital cortex is proposed to play a critical role in initiating visual aura due to observations that CSD originates in this region [33]. Previous fMRI studies have consistently reported that MwA patients exhibit a stronger blood-oxygen-level-dependent response in the visual cortex to visual stimuli compared to both MwoA patients and HCs [34]. A prior MEG study revealed that migraine patients with persistent aura showed the largest increase in P100m amplitude—a component generated in the primary visual cortex—in response to visual stimuli compared to other migraine subgroups [35]. It has been reported that the extrastriate cortex, which primarily centers on the LC, is the only replicable functional finding in MwA [34]. These findings suggest the LC as a pivotal hub of the mechanisms underlying visual aura. Our findings align with existing reports, suggesting that the visual aura in migraine may be associated with increased excitability of the visual cortex—a state that could predispose the visual cortex to CSD. In addition to abnormalities in the visual cortex, we observed that MwA patients exhibit a significantly higher spectral power in the right TTC compared to both HCs and the MwoA group. The TTC is a key component of the auditory cortex and is primarily involved in processing auditory information [36]. Previous studies have shown that migraine patients exhibit impairments in auditory stimulus processing, as characterized by interictal atypical perception, ictal phonophobia, and sound-triggered attacks [37,38]. A MEG study found that, during migraine attacks, adolescent migraine patients exhibited a reduced amplitude of the M150 component, which is thought to be localized to the primary auditory cortex [39]. Our findings provide further support for more pronounced deficits in auditory processing in MwA compared to MwoA. Consistent with this, a hospital-based survey reported a lower prevalence of phonophobia

in MwoA patients than in MwA patients [40]. Given the present findings, this phenomenon could be attributed to the localized increase in spectral power within the TTC, which also suggests that aberrant activity in this region could serve as a potential biomarker specific to MwA.

The most prominent finding of this study regarding FC is that MwA patients exhibit a distinct pattern of weakened FC in the low-frequency band between the visual cortex and brain regions responsible for memory (entorhinal cortex), emotion (rACC), attention (SPC), motor function (precentral cortex), and self-awareness (precuneus). These results strongly indicate that MwA patients exhibit inherent dysfunction in functional cooperation between primary/higher-order visual cortices and multiple neural networks. Thus, aberrant FC could serve as an objective indicator for assessing disease severity. This widespread cortical hypocommunication may link visual aura to broader brain dysfunction, compromising the ability of cortical interactions to modulate nociception. The entorhinal cortex, a hub for sensory integration and pain modulation [41–43], may filter CSD propagation, thereby influencing neurological deficit occurrence [42]. Our observation of weakened occipital-entorhinal cortex FC in MwA supports failure in this gating mechanism that permits aberrant CSD spread and aura phenomena. Collectively, these findings indicate the entorhinal cortex as a potential therapeutic target for mitigating neurological deficits specifically in MwA. Beyond the individual functions described earlier, the rACC, SPC, precentral cortex, and precuneus are all involved in central pain processing [37,44–48]. Building on previous reports of functional and/or structural alterations in these brain regions among migraine patients [16,37,44,49], our study provides further neuromagnetic evidence substantiating a weakened visuo-nociceptive network in MwA. As this impairment could lead to deficits in pain integration, it may play a critical role in the initiation and persistence of MwA. This specific connectivity pattern represents a potential neuroimaging biomarker for MwA that could inform targeted therapeutic strategies for this patient subgroup. For example, transcranial direct current stimulation (tDCS) over the left primary motor cortex has been shown to effectively alleviate pain in migraine and other central pain conditions [47]. Consistent with prior transcranial magnetic stimulation findings of motor cortex hyperexcitability in MwA [50], our findings implicate the precentral cortex in its pathophysiology. The left precentral cortex could be explored as a tDCS target for MwA, providing a pathway toward a specific and precise therapeutic intervention for this migraine subtype.

4.2 Alterations in Neuromagnetic Activity Specific to MwoA

In contrast to patterns observed in MwA patients, MwoA patients exhibited subtype-specific enhancement of FC in gamma1 bands. Gamma oscillations, implicated in neuronal excitability, sensory integration, and pain processing, are altered in migraine [51], with MEG/EEG studies reporting changes during both resting-state and visual stimulation [51–54]. There is accumulating evidence that the rACC exerts a more prominent role in the pathophysiology of MwoA compared to MwA. Two previous resting-state fMRI investigations reported significantly reduced regional homogeneity and amplitude of low-frequency fluctuation in the rACC in MwoA patients, which may reflect long-term impaired affective pain processing and dysfunction of the endogenous analgesic system [44,55]. Proton magnetic resonance spectroscopy studies further revealed subtype-specific patterns of gamma-aminobutyric acid (GABA) reduction in migraine: occipital decreases were specific to MwA, whereas MwoA was characterized by a reduced GABA+/Cr ratio in the ACC, suggesting its critical role in MwoA pathogenesis [56–58]. The cuneus contributes to bottom-up visuospatial attention and, through somatosensory integration, participates in higher cognition processes like consciousness and episodic memory [59,60]. A previous study utilizing machine learning models combined with fMRI identified the cuneus as one of the most discriminative brain regions for distinguishing between MwA and MwoA groups [61]. Our findings suggest aberrant FC between the visual cortex and ACC as a potential neurobiological mechanism underlying MwoA. This aberrant connectivity appears to become more pronounced with disease progression, offering valuable insights for the development of targeted and personalized therapeutic strategies. A previous resting-state fMRI study also reported abnormal causal connectivity within the ACC-visual cortex circuit in MwoA and further demonstrated that this aberrant FC could predict treatment response to non-steroidal anti-inflammatory drugs [62]. Similarly, our finding of abnormal FC between the visual cortex and rACC in MwoA patients may represent a neuromagnetic biomarker that could guide clinical decision-making for pharmacological management in this migraine subpopulation.

4.3 Alterations in Neuromagnetic Activity Shared Between MwA and MwoA

In addition to subtype-specific alterations, we identified aberrant FC common to the MwA and MwoA groups that may represent a shared pathophysiological basis of migraine disorder.

The insula is involved in pain perception [63] while the PCC contributes to processing nociceptive signals and modulating chronic pain pathways [64]. Both regions constitute key elements of the pain matrix [65]. Moreover, they are among the sites most robustly identified as exhibiting altered FC in migraine. Prior MEG and fMRI studies have reported enhanced cuneus-insula FC in MwoA [51,66], and a systematic review further associates PCC-visual region FC with migraine pain intensity [67]. These findings may lend further support to the concept of central hyperexcitability in pain-processing brain regions during the interictal

period. Furthermore, our finding of a significant correlation between aberrant connectivity and headache attack frequency reinforces the notion of migraine as a progressive disorder. Regardless of aura status, migraine patients likely exhibit widespread dysregulation within neuronal networks responsible for sensory integration and processing. These shared alterations constitute a common neural substrate underlying migraine disorder.

4.4 Study Limitations

This study is subject to several limitations that should be noted. First, we acknowledge the modest sample size, which is an inherent challenge in MEG studies that may affect statistical power [14]. Given the substantially lower prevalence of patients diagnosed with migraine with visual aura compared to MwoA, recruitment and acquisition of MEG data for this migraine subtype were more challenging. Future studies should recruit a larger sample to validate our findings. Second, we exclusively enrolled patients with visual aura, which precluded analysis of patients with other aura subtypes. Consequently, future studies should specifically aim to recruit migraine patients with different aura subtypes to facilitate comprehensive subgroup analyses. Third, given the exploratory nature of this study, we adopted a relatively lenient strategy for multiple comparison correction (e.g., by not applying correction at the whole-brain level) to reduce the risk of Type II errors (false negatives), aiming to preliminarily identify potentially meaningful connectivity patterns. We acknowledge that this approach may have increased the risk of Type I errors (false positives) to some extent. Therefore, these findings should be regarded as preliminary evidence. Future studies are needed to validate these preliminary findings in independent samples using stricter corrections, such as the false discovery rate (FDR for ROIs/connections). Finally, given the cross-sectional nature of this study, we cannot establish whether the observed visual network abnormalities represent a predisposing cause or a consequence of recurrent migraine attacks. Future studies employing longitudinal designs are needed to address this question.

5. Conclusions

Overall, this study indicates that MwA and MwoA patients demonstrate distinct patterns of neuromagnetic activity within specific frequency bands. MwA is associated with increased neuromagnetic source strength in visual and auditory cortices and decreased FC within visual networks, whereas MwoA exhibits increased FC within the ACC-visual cortex circuit. These differences suggest unique neurophysiological mechanisms underlying these two migraine subtypes and could serve as functional neurobiomarkers for distinguishing MwA from MwoA, thus providing novel therapeutic targets for distinct migraine subtypes.

Availability of Data and Materials

The original contributions presented in this study are included in the article, further inquiries can be directed to the corresponding author.

Author Contributions

DW, HL, and XW designed the research study. DW and HL performed the research. DW, ZZ and QC performed the experiments and acquired the raw data. DW, ZZ and YY analyzed the data. DW and XW wrote the manuscript. All authors contributed to editorial changes in themanuscript. All authors read and approved the final manuscript. All authors haveparticipated sufficiently in the work and agreed to be accountable for all aspects of the work.

Ethics Approval and Consent to Participate

Ethics approval was provided by the Affiliated Brain Hospital of Nanjing Medical University's Human Research Ethics Committee (2016-KY023). All participants provided written informed consent. This study was conducted in accordance with the ethical guidelines of the Declaration of Helsinki.

Acknowledgment

The authors gratefully acknowledge the support of Department of Neurology, the Affiliated Brain Hospital of Nanjing Medical University.

Funding

This study was supported by the National Key Research and Development Program of China (Grant number 2023YFC2508702); and National Nature Science of China (Grant number 81271440).

Conflict of Interest

The authors declare no conflict of interest.

Supplementary Material

Supplementary material associated with this article can be found, in the online version, at https://doi.org/10.31083/JIN49083.

References

[1] Headache Classification Committee of the International Headache Society (IHS) The International Classification of Headache Disorders, 3rd edition. Cephalalgia. 2018; 38: 1–211. https://doi.org/10.1177/0333102417738202.

[2] Kelman L. The aura: a tertiary care study of 952 migraine patients. Cephalalgia. 2004; 24: 728–734. https://doi.org/10.1111/j.1468-2982.2004.00748.x.

[3] Dodick DW. A Phase-by-Phase Review of Migraine Pathophysiology. Headache. 2018; 58: 4–16. https://doi.org/10.1111/head.13300.

[4] Grodzka O, Dzagoevi K, Rees T, Cabral G, Chądzyński P, Di Antonio S, *et al*. Migraine with and without aura-two distinct entities? A narrative review. The Journal of Headache and Pain. 2025; 26: 77. https://doi.org/10.1186/s10194-025-01998-1.

[5] Gaist D, Hougaard A, Garde E, Reislev NL, Wiwie R, Iversen P, *et al*. Migraine with visual aura associated with thicker visual cortex. Brain. 2018; 141: 776–785. https://doi.org/10.1093/brain/awx382.

[6] Zhang X, Zhou J, Guo M, Cheng S, Chen Y, Jiang N, *et al*. A systematic review and meta-analysis of voxel-based morphometric studies of migraine. Journal of Neurology. 2023; 270: 152–170. https://doi.org/10.1007/s00415-022-11363-w.

[7] Szabó N, Faragó P, Király A, Veréb D, Csete G, Tóth E, *et al*. Evidence for Plastic Processes in Migraine with Aura: A Diffusion Weighted MRI Study. Frontiers in Neuroanatomy. 2017; 11: 138. https://doi.org/10.3389/fnana.2017.00138.

[8] Fu T, Gao Y, Huang X, Zhang D, Liu L, Wang P, *et al*. Brain connectome-based imaging markers for identifiable signature of migraine with and without aura. Quantitative Imaging in Medicine and Surgery. 2024; 14: 194–207. https://doi.org/10.21037/qims-23-827.

[9] Datta R, Aguirre GK, Hu S, Detre JA, Cucchiara B. Interictal cortical hyperresponsiveness in migraine is directly related to the presence of aura. Cephalalgia. 2013; 33: 365–374. https://doi.org/10.1177/0333102412474503.

[10] Coppola G, Di Lorenzo C, Parisi V, Lisicki M, Serrao M, Pierelli F. Clinical neurophysiology of migraine with aura. The Journal of Headache and Pain. 2019; 20: 42. https://doi.org/10.1186/s10194-019-0997-9.

[11] van den Hoek TC, Perenboom MJL, Terwindt GM, Tolner EA, van de Ruit M. Bi-sinusoidal light stimulation reveals an enhanced response power and reduced phase coherence at the visual cortex in migraine. Frontiers in Neurology. 2023; 14: 1274059. https://doi.org/10.3389/fneur.2023.1274059.

[12] Abbas Abdulhussein M, Alyasseri ZAA, Mohammed HJ, An X. Lack of Habituation in Migraine Patients Based on High-Density EEG Analysis Using the Steady State of Visual Evoked Potential. Entropy. 2022; 24: 1688. https://doi.org/10.3390/e24111688.

[13] Pikor D, Banaszek-Hurla N, Drelichowska A, Hurla M, Dorszewska J, Wolak T, *et al*. fMRI Insights into Visual Cortex Dysfunction as a Biomarker for Migraine with Aura. Neurology International. 2025; 17: 15. https://doi.org/10.3390/neurolint17020015.

[14] Gopalakrishnan R, Malan NS, Mandava N, Dunn EJ, Nero N, Burgess RC, *et al*. Magnetoencephalography studies in migraine and headache disorders: A systematic review. Headache. 2025; 65: 353–366. https://doi.org/10.1111/head.14867.

[15] Baillet S. Magnetoencephalography for brain electrophysiology and imaging. Nature Neuroscience. 2017; 20: 327–339. https://doi.org/10.1038/nn.4504.

[16] Zhang X, Xu F, Wu D, Wang Y, Chen Q, Sun F, *et al*. Altered Neuromagnetic Activity in the Default Mode Network in Migraine and Its Subgroups (Episodic Migraine and Chronic Migraine). Journal of Integrative Neuroscience. 2024; 23: 19. https://doi.org/10.31083/j.jin2301019.

[17] Nieboer D, Sorrentino P, Hillebrand A, Heymans MW, Twisk JWR, Stam CJ, *et al*. Brain Network Integration in Patients with Migraine: A Magnetoencephalography Study. Brain Connectivity. 2020; 10: 224–235. https://doi.org/10.1089/brain.2019.0705.

[18] Tadel F, Bock E, Niso G, Mosher JC, Cousineau M, Pantazis D, *et al*. MEG/EEG Group Analysis With Brainstorm. Frontiers in Neuroscience. 2019; 13: 76. https://doi.org/10.3389/fnins.2019.00076.

[19] Florin E, Baillet S. The brain's resting-state activity is shaped by synchronized cross-frequency coupling of neural oscillations. NeuroImage. 2015; 111: 26–35. https://doi.org/10.1016/j.neuroimage.2015.01.054.

[20] Kanamori Y, Shigeto H, Hironaga N, Hagiwara K, Uehara T, Chatani H, *et al*. Minimum norm estimates in MEG can delineate the onset of interictal epileptic discharges: A comparison with ECoG findings. NeuroImage. Clinical. 2013; 2: 663–669. https://doi.org/10.1016/j.nicl.2013.04.008.

[21] Hincapié AS, Kujala J, Mattout J, Daligault S, Delpuech C, Mery D, *et al*. MEG Connectivity and Power Detections with Minimum Norm Estimates Require Different Regularization Parameters. Computational Intelligence and Neuroscience. 2016; 2016: 3979547. https://doi.org/10.1155/2016/3979547.

[22] Gramfort A, Luessi M, Larson E, Engemann DA, Strohmeier D, Brodbeck C, *et al*. MNE software for processing MEG and EEG data. NeuroImage. 2014; 86: 446–460. https://doi.org/10.1016/j.neuroimage.2013.10.027.

[23] Desikan RS, Ségonne F, Fischl B, Quinn BT, Dickerson BC, Blacker D, *et al*. An automated labeling system for subdividing the human cerebral cortex on MRI scans into gyral based regions of interest. NeuroImage. 2006; 31: 968–980. https://doi.org/10.1016/j.neuroimage.2006.01.021.

[24] Niso G, Tadel F, Bock E, Cousineau M, Santos A, Baillet S. Brainstorm Pipeline Analysis of Resting-State Data From the Open MEG Archive. Frontiers in Neuroscience. 2019; 13: 284. https://doi.org/10.3389/fnins.2019.00284.

[25] Colclough GL, Woolrich MW, Tewarie PK, Brookes MJ, Quinn AJ, Smith SM. How reliable are MEG resting-state connectivity metrics? NeuroImage. 2016; 138: 284–293. https://doi.org/10.1016/j.neuroimage.2016.05.070.

[26] Colclough GL, Brookes MJ, Smith SM, Woolrich MW. A symmetric multivariate leakage correction for MEG connectomes. NeuroImage. 2015; 117: 439–448. https://doi.org/10.1016/j.neuroimage.2015.03.071.

[27] Brookes MJ, Hale JR, Zumer JM, Stevenson CM, Francis ST, Barnes GR, *et al*. Measuring functional connectivity using MEG: methodology and comparison with fcMRI. NeuroImage. 2011; 56: 1082–1104. https://doi.org/10.1016/j.neuroimage.2011.02.054.

[28] Cheng CH, Wang PN, Mao HF, Hsiao FJ. Subjective cognitive decline detected by the oscillatory connectivity in the default mode network: a magnetoencephalographic study. Aging. 2020; 12: 3911–3925. https://doi.org/10.18632/aging.102859.

[29] Godfrey M, Singh KD. Measuring robust functional connectivity from resting-state MEG using amplitude and entropy correlation across frequency bands and temporal scales. NeuroImage. 2021; 226: 117551. https://doi.org/10.1016/j.neuroimage.2020.117551.

[30] Grill-Spector K, Kourtzi Z, Kanwisher N. The lateral occipital complex and its role in object recognition. Vision Research. 2001; 41: 1409–1422. https://doi.org/10.1016/s0042-6989(01)00073-6.

[31] Hubbard CS, Becerra L, Smith JH, DeLange JM, Smith RM, Black DF, *et al*. Brain Changes in Responders vs. Non-Responders in Chronic Migraine: Markers of Disease Reversal. Frontiers in Human Neuroscience. 2016; 10: 497. https://doi.org/10.3389/fnhum.2016.00497.

[32] Niddam DM, Lai KL, Hsiao YT, Wang YF, Wang SJ. Grey-matter network topology in migraine with aura. Cephalalgia. 2025; 45: 3331024251353146. https://doi.org/10.1177/03331024251353146.

[33] Hadjikhani N, Sanchez Del Rio M, Wu O, Schwartz D, Bakker D, Fischl B, *et al*. Mechanisms of migraine aura revealed by functional MRI in human visual cortex. Proceedings of the National Academy of Sciences of the United States of America. 2001; 98: 4687–4692. https://doi.org/10.1073/pnas.071582498.

[34] Russo A, Silvestro M, Tessitore A, Tedeschi G. Recent Insights in Migraine With Aura: A Narrative Review of Advanced Neuroimaging. Headache. 2019; 59: 637–649. https://doi.org/10.1111/head.13512.

[35] Chen WT, Lin YY, Fuh JL, Hämäläinen MS, Ko YC, Wang SJ. Sustained visual cortex hyperexcitability in migraine with persistent visual aura. Brain. 2011; 134: 2387–2395. https://doi.org/10.1093/brain/awr157.

[36] Nakai Y, Jeong JW, Brown EC, Rothermel R, Kojima K, Kambara T, *et al*. Three- and four-dimensional mapping of speech and language in patients with epilepsy. Brain. 2017; 140: 1351–1370. https://doi.org/10.1093/brain/awx051.

[37] Guarnera A, Bottino F, Napolitano A, Sforza G, Cappa M, Chioma L, *et al*. Early alterations of cortical thickness and gyrification in migraine without aura: a retrospective MRI study in pediatric patients. The Journal of Headache and Pain. 2021; 22: 79. https://doi.org/10.1186/s10194-021-01290-y.

[38] Harriott AM, Schwedt TJ. Migraine is associated with altered processing of sensory stimuli. Current Pain and Headache Reports. 2014; 18: 458. https://doi.org/10.1007/s11916-014-0458-8.

[39] Korostenskaja M, Pardos M, Kujala T, Rose DF, Brown D, Horn P, *et al*. Impaired auditory information processing during acute migraine: a magnetoencephalography study. The International Journal of Neuroscience. 2011; 121: 355–365. https://doi.org/10.3109/00207454.2011.560312.

[40] Tu YH, Wang YF, Yuan H, Chen SP, Tzeng YS, Chen WT, *et al*. Most bothersome symptoms in patients with migraine: A hospital-based study in Taiwan. Headache. 2022; 62: 596–603. https://doi.org/10.1111/head.14308.

[41] Herber CS, Pratt KJB, Shea JM, Villeda SA, Giocomo LM. Spatial coding dysfunction and network instability in the aging medial entorhinal cortex. Nature Communications. 2025; 16: 8770. https://doi.org/10.1038/s41467-025-63229-0.

[42] Martens-Mantai T, Speckmann EJ, Gorji A. Propagation of cortical spreading depression into the hippocampus: The role of the entorhinal cortex. Synapse. 2014; 68: 574–584. https://doi.org/10.1002/syn.21769.

[43] Schwedt TJ, Chong CD, Wu T, Gaw N, Fu Y, Li J. Accurate Classification of Chronic Migraine via Brain Magnetic Resonance Imaging. Headache. 2015; 55: 762–777. https://doi.org/10.1111/head.12584.

[44] Xue T, Yuan K, Cheng P, Zhao L, Zhao L, Yu D, *et al*. Alterations of regional spontaneous neuronal activity and corresponding brain circuit changes during resting state in migraine without aura. NMR in Biomedicine. 2013; 26: 1051–1058. https://doi.org/10.1002/nbm.2917.

[45] Ou Y, Ni X, Gao X, Yu Y, Zhang Y, Wang Y, *et al*. Structural and functional changes of anterior cingulate cortex subregions in migraine without aura: relationships with pain sensation and pain emotion. Cerebral Cortex. 2024; 34: bhae040. https://doi.org/10.1093/cercor/bhae040.

[46] Oshiro Y, Quevedo AS, McHaffie JG, Kraft RA, Coghill RC. Brain mechanisms supporting spatial discrimination of pain. The Journal of Neuroscience. 2007; 27: 3388–3394. https://doi.org/10.1523/JNEUROSCI.5128-06.2007.

[47] Lim M, Kim DJ, Nascimento TD, DaSilva AF. High-definition tDCS over primary motor cortex modulates brain signal variability and functional connectivity in episodic migraine. Clinical Neurophysiology. 2024; 161: 101–111. https://doi.org/10.1016/j.clinph.2024.02.012.

[48] Cavanna AE, Trimble MR. The precuneus: a review of its functional anatomy and behavioural correlates. Brain. 2006; 129: 564–583. https://doi.org/10.1093/brain/awl004.

[49] Ge HT, Liu HX, Xiang J, Miao AL, Tang L, Guan QS, *et al*. Abnormal cortical activation in females with acute migraine: a magnetoencephalography study. Clinical Neurophysiology. 2015; 126: 170–179. https://doi.org/10.1016/j.clinph.2014.03.033.

[50] Yuksel H, Topalkara KK. Increased Cortical Excitability in Female Migraineurs: A Transcranial Magnetic Stimulation Study Conducted in the Preovulatory Phase. Journal of Clinical Neurology. 2021; 17: 236–241. https://doi.org/10.3988/jcn.2021.17.2.236.

[51] Wu D, Zhou Z, Wang Y, Liu H, Yu Y, Chen Q, *et al*. Altered neuromagnetic activity under visual stimuli in migraine: a multi-frequency magnetoencephalography study. Frontiers in Neurology. 2025; 16: 1567150. https://doi.org/10.3389/fneur.2025.1567150.

[52] Li F, Xiang J, Wu T, Zhu D, Shi J. Abnormal resting-state brain activity in headache-free migraine patients: A magnetoencephalography study. Clinical Neurophysiology. 2016; 127: 2855–2861. https://doi.org/10.1016/j.clinph.2016.05.015.

[53] Coppola G, Ambrosini A, Di Clemente L, Magis D, Fumal A, Gérard P, *et al*. Interictal abnormalities of gamma band activity in visual evoked responses in migraine: an indication of thalamocortical dysrhythmia? Cephalalgia. 2007; 27: 1360–1367. https://doi.org/10.1111/j.1468-2982.2007.01466.x.

[54] Lisicki M, D'Ostilio K, Coppola G, Nonis R, Maertens de Noordhout A, Parisi V, *et al*. Headache Related Alterations of Visual Processing in Migraine Patients. The Journal of Pain. 2020; 21: 593–602. https://doi.org/10.1016/j.jpain.2019.08.017.

[55] Yu D, Yuan K, Zhao L, Zhao L, Dong M, Liu P, *et al*. Regional homogeneity abnormalities in patients with interictal migraine without aura: a resting-state study. NMR in Biomedicine. 2012; 25: 806–812. https://doi.org/10.1002/nbm.1796.

[56] Bridge H, Stagg CJ, Near J, Lau CI, Zisner A, Cader MZ. Altered neurochemical coupling in the occipital cortex in migraine with visual aura. Cephalalgia. 2015; 35: 1025–1030. https://doi.org/10.1177/0333102414566860.

[57] Bathel A, Schweizer L, Stude P, Glaubitz B, Wulms N, Delice S, *et al*. Increased thalamic glutamate/glutamine levels in migraineurs. The Journal of Headache and Pain. 2018; 19: 55. https://doi.org/10.1186/s10194-018-0885-8.

[58] Wu X, Han S, Yang Y, Dai H, Wu P, Zhao H, *et al*. Decreased Brain GABA Levels in Patients with Migraine Without Aura: An Exploratory Proton Magnetic Resonance Spectroscopy Study. Neuroscience. 2022; 488: 10–19. https://doi.org/10.1016/j.neuroscience.2022.02.010.

[59] Vanni S, Tanskanen T, Seppä M, Uutela K, Hari R. Coinciding early activation of the human primary visual cortex and anteromedial cuneus. Proceedings of the National Academy of Sciences of the United States of America. 2001; 98: 2776–2780. https://doi.org/10.1073/pnas.041600898.

[60] Chen W, Xie G, Xu C, Liang J, Zhang C. The relationship between regional homogeneity in resting-state functional magnetic resonance imaging and cognitive function in depressive disorders with migraine. Scientific Reports. 2025; 15: 11810. https://doi.org/10.1038/s41598-025-96850-6.

[61] Li G, Yang H, He L, Zeng G. Interpretable Artificial Intelligence Analysis of Functional Magnetic Resonance Imaging for Migraine Classification: Quantitative Study. JMIR Medical Informatics. 2025; 13: e72155. https://doi.org/10.2196/72155.

[62] Wei HL, Yang Q, Zhou GP, Chen YC, Yu YS, Yin X, *et al*. Abnormal causal connectivity of anterior cingulate cortex-visual cortex circuit related to nonsteroidal anti-inflammatory drug efficacy in migraine. The European Journal of Neuroscience. 2024; 59: 446–456. https://doi.org/10.1111/ejn.16219.

[63] Uddin LQ, Nomi JS, Hébert-Seropian B, Ghaziri J, Boucher O. Structure and Function of the Human Insula. Journal of Clinical Neurophysiology. 2017; 34: 300–306. https://doi.org/10.1097/WNP.0000000000000377.

[64] Amaral VCG, Tukamoto G, Kubo T, Luiz RR, Gasparetto E, Vincent MB. Migraine improvement correlates with posterior cingulate cortical thickness reduction. Arquivos De Neuro-Psiquiatria. 2018; 76: 150–157. https://doi.org/10.1590/0004-282x20180004.

[65] Garcia-Larrea L, Peyron R. Pain matrices and neuropathic pain matrices: a review. Pain. 2013; 154: S29–S43. https://doi.org/10.1016/j.pain.2013.09.001.

[66] Hubbard CS, Khan SA, Keaser ML, Mathur VA, Goyal M, Seminowicz DA. Altered Brain Structure and Function Correlate with Disease Severity and Pain Catastrophizing in Migraine Patients. eNeuro. 2014; 1: e20.14. https://doi.org/10.1523/ENEURO.0006-14.2014.

[67] Schramm S, Börner C, Reichert M, Baum T, Zimmer C, Heinen F, *et al*. Functional magnetic resonance imaging in migraine: A systematic review. Cephalalgia. 2023; 43: 3331024221128278. https://doi.org/10.1177/03331024221128278.